nature medicine

A novel peptide CXCR ligand derived from extracellular matrix degradation during airway inflammation

Nathaniel M Weathington[1], Anneke H van Houwelingen[2], Brett D Noerager[1], Patricia L Jackson[1], Aletta D Kraneveld[2], F Shawn Galin[1] Gert Folkerts[2], Frans P Nijkamp[2] & J Edwin Blalock[1]

We describe the tripeptide neutrophil chemoattractant N-acetyl Pro-Gly-Pro (PGP), derived from the breakdown of extracellular matrix (ECM), which shares sequence and structural homology with an important domain on alpha chemokines. PGP caused chemotaxis and production of superoxide through CXC receptors, and administration of peptide caused recruitment of neutrophils (PMNs) into lungs of control, but not CXCR2-deficient mice. PGP was generated in mouse lung after exposure to lipopolysaccharide, and *in vivo* and *in vitro* blockade of PGP with monoclonal antibody suppressed PMN responses as much as chemokine-specific monoclonal antibody. Extended PGP treatment caused alveolar enlargement and right ventricular hypertrophy in mice. PGP was detectable in substantial concentrations in a majority of bronchoalveolar lavage samples from individuals with chronic obstructive pulmonary disease, but not control individuals. Thus, PGP's activity links degradation of ECM with neutrophil recruitment in airway inflammation, and PGP may be a biomarker and therapeutic target for neutrophilic inflammatory diseases.

Neutrophils are effectors in pulmonary inflammatory diseases, including chronic obstructive pulmonary disease (COPD) and acute lung injury[1]. PMNs are required for pulmonary symptoms arising from trauma and hemorrhage or lipopolysaccharide (LPS), as their depletion eliminates the phenotype[2]. The major chemoattractants for neutrophils during inflammation are Glu-Leu-Arg motif–containing ELR$^+$ CXC chemokines[3] including IL-8 (CXCL8) and GRO-α, GRO-β and GRO-γ (CXCL1, CXCL2 and CXCL3, respectively) in humans and KC and MIP-2 (CXCL1 and CXCL2) in mice. The receptors for these molecules are CXCR1 and CXCR2 in humans[4,5] and only CXCR2 in mice[6].

Others have reported chemotactic activities of ECM- or collagen-derived peptides[7–10] without description of a molecular mechanism for such activity. The PGP peptide was discovered in a rabbit model investigating alkali injury to the eye, where PMN inflammation leads to corneal ulceration and perforation. It was shown that alkali treatment of cornea generates PGP, probably from collagen[11,12]; the peptide is chemotactic for neutrophils; and corneal peptide treatment causes neutrophilia similar to that seen in alkali injury[13].

Similarly, collagen peptides are active in lung. Intratracheal administration of collagen fragments causes accumulation of pulmonary neutrophils[14], whereas overexpression of collagenase-1 (ref. 15) or blockade of matrix metalloproteinases (MMPs)[16] causes emphysema and attenuates symptoms of COPD, respectively. Airway exposure of mice to LPS causes a pathology in which MMP-9 activity and lung neutrophil burden correlate highly[17].

Here we sought the specific molecular mechanism of PGP's activity on neutrophils and evaluated its relevance to lung pathology. We structurally compared PGP with CXCL, characterized PGP's activity on human and mouse PMNs and CXCR transfectants, and tested receptor binding. *In vivo*, we tested PGP's effects on airway cell distributions in normal and CXCR2-deficient (*Cxcr2*$^{-/-}$) mice, and characterized the presence and activity of PGP *in situ* in pulmonary inflammation caused by exposure to LPS. We tested whether long-term exposure to PGP caused pathology by monitoring alveolar enlargement and right ventricular hypertrophy. Finally, we assayed BAL samples from individuals with COPD and control individuals for PGP.

RESULTS

PGP is chemotactic for neutrophils *in vivo* and *in vitro*

In initial *in vivo* experiments, we exposed 6–8-week-old C57 Bl/6J mice to synthetic, highly purified, endotoxin-free PGP or control peptide Pro-Gly-Gly (PGG) in sterile hospital-grade phosphate-buffered saline (PBS) or PBS alone by intratracheal administration. We killed the mice 5 h later, performed bronchoalveolar lavage (BAL), and differentially counted airway cells. PGP caused a marked increase in the total number of cells in lungs of PGP- but not PGG-exposed mice (**Fig. 1a**); this increase is completely accounted for by the rise in neutrophil numbers, with other cell types unaffected by either peptide, and BALB/c mice responded similarly (data not shown). Thus, PGP causes specific PMN recruitment into the airways.

To systematically evaluate the effects of PGP on neutrophils, we used a transwell chemotaxis system with purified PMNs or neutrophil-like differentiated HL-60 cells placed in media above a 3 μm polycarbonate filter, and PGP, chemokines or media placed in

[1]Department of Physiology and Biophysics, University of Alabama at Birmingham, 1918 University Boulevard, Birmingham, Alabama 35294, USA. [2]Utrecht Institute for Pharmaceutical Sciences, Department of Phamacology and Pathophysiology, Utrecht University, Sorbonnelaan 16, 3584 CA Utrecht, The Netherlands. Correspondence should be addressed to J.E.B. (blalock@uab.edu).

Received 19 September 2005; accepted 27 December 2005; published online 12 February 2006; doi:10.1038/nm1361

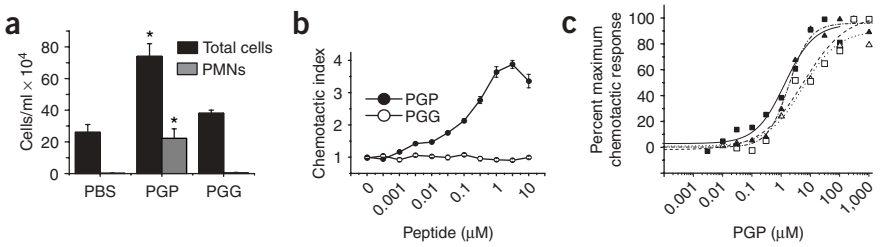

Figure 1 PGP is chemotactic for PMNs *in vitro* and *in vivo*. (**a**) The PGP peptide, but not the PGG control peptide causes an increase in airway PMNs after intratracheal administration (250 μg in 50 μl) to 6–8-week-old C57 BL/6J mice; BAL and differential cell counts were performed 5 h after treatment (*$P < 0.05$ compared to PBS group). (**b**) PGP is a chemoattractant of human PMNs in an *in vitro* transwell chemotaxis assay, whereas PGG had no chemotactic activity; 2×10^5 PMNs were placed on one side of a 3 μm filter with peptides present on the other side, and migrated cells were photographed and quantified after 1 h at 37 °C. (**c**) Dose-response curves for human PMNs (open squares), HL-60 cells (filled squares), bone marrow–derived mouse PMNs (open triangles) and mouse peritoneal PMNs (filled triangles).

the lower chamber. After 1 h, we quantified migration and indexed it to basal (media control) activity. PGP was chemotactic for neutrophils between 10 nM and 100 μM, and PGG had no activity, consistent with the *in vivo* data (**Fig. 1b**). PGP was active on purified PMNs from humans and mice as well as HL-60 cells[18], with 50% effective concentration (EC_{50}) values from 0.5 to 6 μmol for all cells tested (**Fig. 1c**). PGP is chemotactic rather than chemokinetic, as disruption of the PGP gradient between chambers suppressed cell migration. IL-8–dependent chemotaxis was similarly disrupted by PGP in the upper chamber (**Supplementary Fig. 1** online).

PGP has structural homology to CXC chemokines

Searching for a mechanism for the activity of PGP and other collagen-derived peptides, we looked for similarity between them and the CXC chemokines classically defined as inflammatory neutrophil chemoattractants. Sequence comparison of a collagen fragment isolated using the 9A4 antibody, which recognizes the PPGPQ sequence[19], to chemokine sequences showed that several ELR^+ CXC chemokines (CXCL1, CXCL2 and CXCL3 of human, mouse and rat) contain a conserved PPGPH sequence immediately N-terminal to the third structural cysteine. IL-8 has the sequence ESGPH in this position (**Fig. 2a**), and none of the ELR^- CXC or CC chemokines possess this 'GP' motif seen in all neutrophil-specific chemokines. Earlier structure-function studies of IL-8 showed that this GP motif was an absolute requirement for neutrophil cell binding and activation in radioligand and elastase release assays, respectively[20].

We next compared the available structures of IL-8 (ref. 21) and PGP[22] and found that the molecular orientation of the SGP motif of IL-8 is well represented in the structure of the predominant 'all-*trans*' isomer of PGP (**Fig. 2b,c**). In IL-8, the SGP motif (**Fig. 2d**) follows the first of three β-strands and resides in the so-called '30s loop' of the molecule, which is in close proximity to the ELR domain (**Fig. 2d**). These domains are exposed to solvent and linked by the bridging disulfide immediately C-terminal to each (**Fig. 2d**). Moreover, the SGP region of IL-8 is alone active as a chemoattractant with dosimetry similar to PGP (**Supplementary Fig. 1** online).

PGP activity is mediated by CXCR1 and CXCR2

To test whether PGP and IL-8 act on a common receptor, we used monoclonal antibodies targeting the CXCR1 and CXCR2 receptors abundant on human PMNs. Incubating PMNs with a mixture of antibodies to these receptors predictably suppressed IL-8–dependent chemotaxis to control levels (**Fig. 3a**). When we evaluated PGP-dependent chemotaxis, pretreatment with the same antibodies

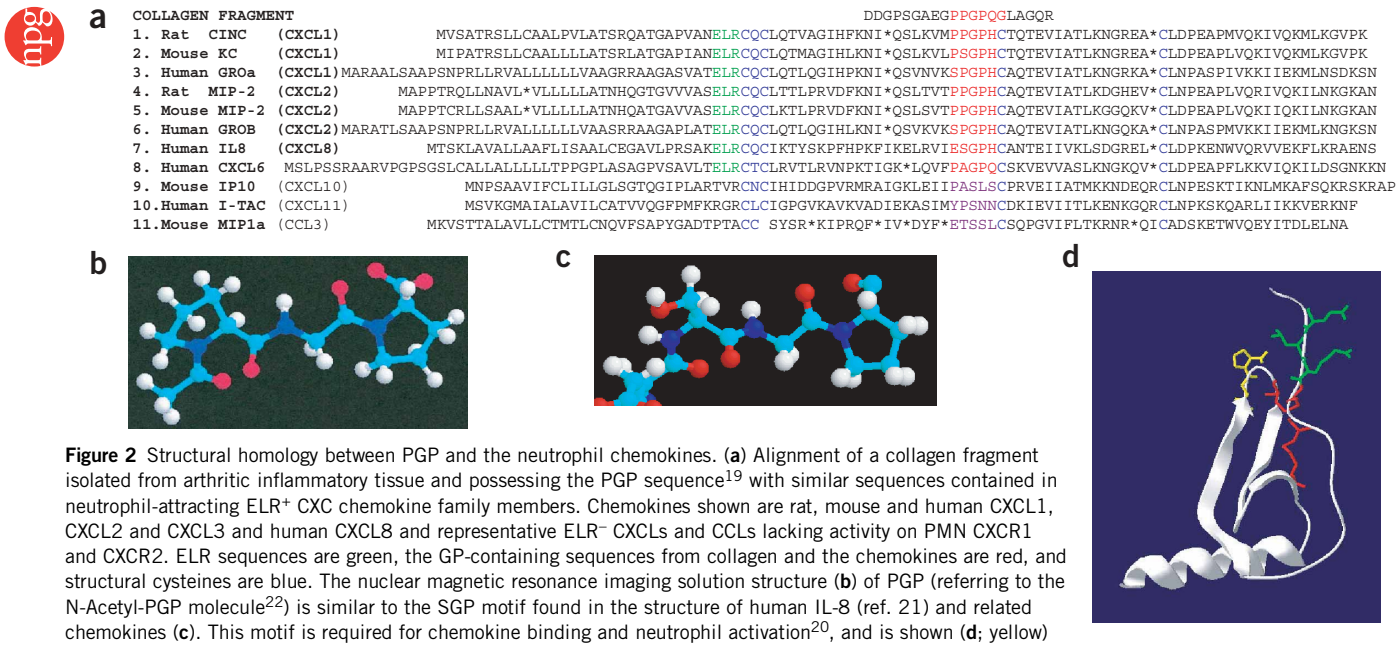

Figure 2 Structural homology between PGP and the neutrophil chemokines. (**a**) Alignment of a collagen fragment isolated from arthritic inflammatory tissue and possessing the PGP sequence[19] with similar sequences contained in neutrophil-attracting ELR^+ CXC chemokine family members. Chemokines shown are rat, mouse and human CXCL1, CXCL2 and CXCL3 and human CXCL8 and representative ELR^- CXCLs and CCLs lacking activity on PMN CXCR1 and CXCR2. ELR sequences are green, the GP-containing sequences from collagen and the chemokines are red, and structural cysteines are blue. The nuclear magnetic resonance imaging solution structure (**b**) of PGP (referring to the N-Acetyl-PGP molecule[22]) is similar to the SGP motif found in the structure of human IL-8 (ref. 21) and related chemokines (**c**). This motif is required for chemokine binding and neutrophil activation[20], and is shown (**d**; yellow) to be solution accessible in the IL-8 structure and close in space to the important ELR motif (green) present in the neutrophil specific CXC chemokines. For reference, the structural cysteines are shown in red.

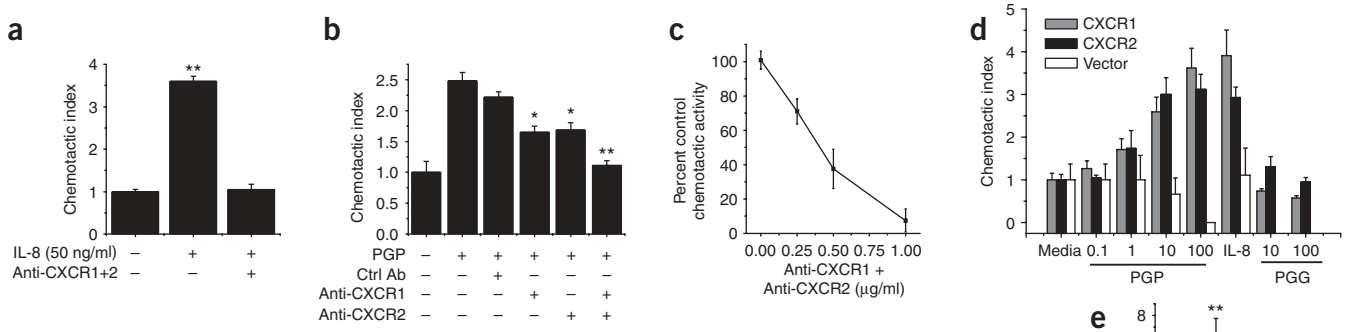

Figure 3 PMN chemotaxis to PGP is dependent on the CXC chemokine receptors. (**a**,**b**) PMNs were incubated with 1 μg/ml monoclonal antibody against CXCR1, CXCR2, both or 2 μg/ml IgG2a isotype control for 1 h at 22 °C before assaying chemotaxis to 50 ng/ml IL-8 (**a**) or 100 μg/ml PGP (**b**). (**c**) The dose-response curve for the inhibition of PGP-mediated PMN chemotaxis with monoclonal antibodies against both CXCR1 and CXCR2. (**d**) RBL cells stably transfected to express CXCR1 or CXCR2 migrate to PGP (μg/ml as indicated, $P < 0.05$ for CXCR1 and CXCR2 at 10 and 100) and IL-8 (50 ng/ml), but not PGG, whereas vector-transfected controls are unresponsive to either ligand. (**e**) *Cxcr2*$^{-/-}$ mice and BALB/c control mice ($n = 5$ per group) were intratracheally administered 250 μg PGP in 50 μl PBS or PBS alone. BAL and cell counts were performed 5 h later; because *Cxcr2*$^{-/-}$ mice are smaller than controls, PMN counts are shown indexed to the values for PBS-treated mice from each group, rather than absolute PMN numbers, which are (left to right) 5.3 and 34.9 for wild-type mice and 2.1 and 2.4 for knockout mice (PMN × 10^4 per ml BAL fluid). *$P < 0.05$, **$P < 0.01$ compared to controls by *t*-tests in **a**,**d** and **e**; ANOVA in **b**.

also completely suppressed neutrophil chemotaxis, whereas each antibody alone partially suppressed migration (**Fig. 3b**). This effect was dose dependent, with a 50% inhibitory concentration (IC_{50}) of approximately 0.4 μg/ml (**Fig. 3c**), consistent with IL-8 dosages and manufacturer's specifications. We then assayed production of superoxide resulting from CXCR1 ligation[23], and showed that both IL-8 and PGP cause release of superoxide from human PMNs, with PGP pretreatment desensitizing cells to IL-8– but not formyl Met-Leu-Phe (fMLP)-dependent production of superoxide, indicating the action of PGP on CXCR1 (**Supplementary Fig. 1** online).

Assaying the presumptive binding of PGP to CXCR1 and CXCR2, we performed receptor competition assays with ^{125}I-radiolabeled IL-8 on cells from the rat basophilic leukemia (RBL) cell line stably transfected with the CXCR1 and CXCR2 receptors[24]. Excess unlabeled IL-8 markedly suppressed the specific binding of radiolabeled IL-8, and this specific binding is also blocked in the presence of unlabeled PGP (**Supplementary Fig. 1** online). Because the CXCR1- and CXCR2-transfected RBL cells are each chemotactic for IL-8 (ref. 24), PGP can likewise act as a chemoattractant for both, whereas vector-only RBL transfectants are unresponsive to PGP and IL-8 (**Fig. 3d**). The PGG peptide had no effect on migration of CXCR transfectants. Collectively, these data show that, like IL-8, PGP can act on both CXCR1 and CXCR2.

Testing whether PGP's activity was dependent on chemokine receptors *in vivo*, we intratracheally administered PGP to *Cxcr2*$^{-/-}$ mice[6] (on the BALB/c background). In contrast to normal BALB/c mice, the PGP-treated *Cxcr2*$^{-/-}$ mice did not accumulate PMNs in the airway compared to PBS-treated mice (**Fig. 3e**).

PGP is produced *in vivo* in the lung after exposure to LPS

We attempted to measure PGP in BAL samples from inflamed airways, obtained at different times after exposure to aerosolized LPS. By developing a highly sensitive electrospray ionization–liquid chromatography–mass spectrometry (ESI-LC-MS/MS) protocol, we were able specifically detect and quantify the amount of PGP. **Supplementary Figure 2** online shows the ESI-LC-MS/MS profile for a PGP standard and that of the peptide produced endogenously in response to LPS. PGP eluted from liquid chromatography at 6 min with a molecular weight of 312, and was fragmented in a collision chamber to yield daughter ions with molecular weights of 112 and 140, which can be used to generate a standard curve (**Supplementary Fig. 2** online). Monitoring this profile let us quantify PGP in BAL fluids taken after exposure to LPS, whereas BAL fluids from unchallenged mice did not contain PGP (**Supplementary Fig. 2** online).

The chronology of cells and mediators involved in the neutrophilic response to airway exposure to LPS progressed as follows (**Fig. 4a**). In the first 6 h, neutrophil chemokines KC and MIP-2 (CXCL1 and CXCL2, respectively) were produced at high levels, and neutrophils had begun to infiltrate the airway. Between 6 and 12 h after exposure, PMN cell numbers continued to increase though chemokine concentrations declined substantially. During this time, the PGP peptide became detectable in nanogram amounts, and 12 h after LPS exposure, PGP concentrations had risen to more than 800-fold molar excess to KC. To estimate the *in vivo* PGP concentration in the airway surface liquid, we used a previously described technique[25], comparing the concentrations of freely permeant urea in BAL fluid and serum, and found the dilution factor of BAL to be ~77-fold, indicating that PGP was present at a peak concentration of ~231 ng/ml or ~0.7 μM (KC is ~7 ng/ml or ~0.8 nM at this time point). The neutrophil numbers and PGP concentrations remained high until the 24 h time point. From 24 to 48 h after exposure, airway neutrophil numbers declined as the PGP peptide signal disappeared.

PGP peptides in the LPS-treated lung act on PMNs

To determine whether the PGP detected in mouse BAL fluids contributed to the recruitment of PMNs, we monitored clearance of PGP from the airway after intratracheal administration of 100 μg of peptide, and observed rapid depletion of free PGP in BAL fluids within 2 h (**Supplementary Fig. 3** online). At a time when PMN influx was observed (that is, 6 h after PGP treatment; **Fig. 1a**), peptide concentration was similar to that seen in response to inhalation of LPS (5 versus 3 ng/ml, respectively). To directly test the biological activity of PGP in this model, we evaluated chemotactic activity of BAL fluids from LPS-exposed mice on neutrophils. We used monoclonal antibodies specific for PGP and chemokines to differentially block chemotaxis. The monoclonal antibody 9A4 (refs. 19,26)

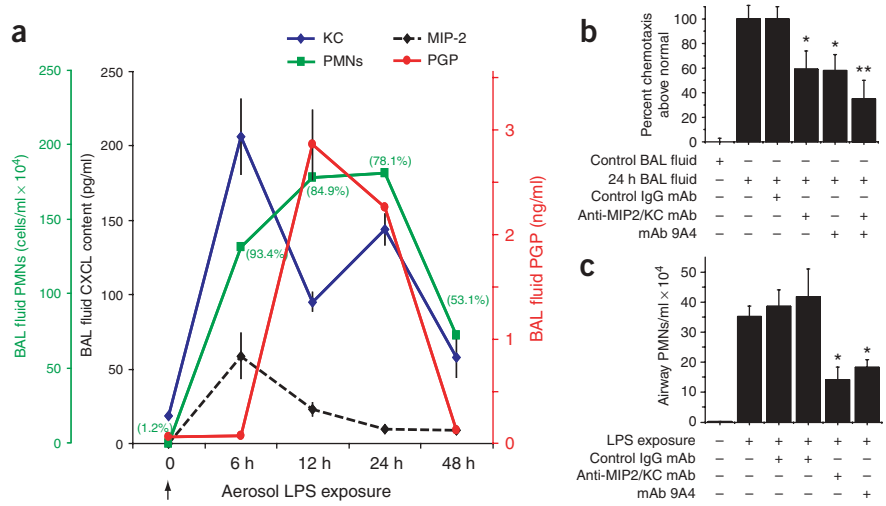

Figure 4 Kinetics of neutrophil influx, CXC chemokine and PGP production in the mouse airway after exposure to aerosolized LPS (**a**). Monoclonal antibodies against KC and MIP-2 or PGP inhibit *in vitro* PMN chemotaxis caused by bronchoalveolar lavage fluids from LPS-exposed mice (**b**), and decrease the *in vivo* neutrophil burden in lungs of LPS-exposed BALB/c mice (**c**). (**a**) Mice were exposed to 100 μg/ml aerosolized LPS for 1 h at time 0. BAL samples ($n = 3$ per time point) were collected and analyzed for neutrophil number (green squares, outer left axis; numbers are percentage of PMNs of total cells); KC and MIP-2 chemokine concentrations by ELISA (blue diamonds and black triangles, respectively, inner left axis); and PGP (red circles, right axis) by ESI-LC-MS/MS. (**b**) Twenty-four hours after LPS exposure, BAL samples were collected, and supernatants were incubated for 1 h with monoclonal antibodies against KC (50 μg/ml), MIP-2 (50 μg/ml), PGP (9A4, 5 μg/ml) or isotype control antibody (50 μg/ml) before PMN chemotaxis. Scale shows activity of BAL samples from LPS-exposed mice versus LPS-naive mice, showing mean ± s.e.m. from six mice. (**c**) Mice exposed to aerosolized LPS were intratracheally administered PBS, isotype control monoclonal antibody (50 μg total), monoclonal antibody against MIP-2 and KC (25 μg each) or monoclonal antibody 9A4 (30 μg) in 35 μl PBS 1 and 10 h after LPS. PMNs were counted from 24 h BAL samples ($n = 3$ per group); isotype controls IgG2a (third bar) and IgG1 (fourth bar) are controls for MIP2- and KC-specific antibody and 9A4 antibody, respectively. $^*P < 0.05$, $^{**}P < 0.01$ compared to positive controls by ANOVA for **b** and **c**.

recognizes the collagen sequence GPPGPQ, which is only exposed after proteolysis of collagen, and specifically inhibits PGP chemotactic activity. Coincubation of 9A4 with chemoattractants potently blocked chemotaxis to PGP, but not to IL-8, KC or MIP2 (**Supplementary Fig. 3** online).

A 1-h preincubation of BAL fluids taken 24 h after exposure to LPS with either 9A4 or monoclonal antibody specific for KC and MIP-2 markedly reduced (~40%) chemotaxis to the BAL fluid, and when the antibodies were used in combination, chemotaxis was further suppressed (~65% decrease; **Fig. 4b**), suggesting that PGP-containing peptides and chemokines independently and additively affect PMN traffic 24 h after LPS challenge.

We then tested whether 9A4 or monoclonal antibody specific for MIP-2 and KC could block LPS-dependent neutrophil infiltration of the lung *in vivo*. These antibodies, when intratracheally administered 1 and 10 h after exposure to LPS, similarly reduced the neutrophil burden in the lungs of mice 24 h after exposure to LPS compared to appropriate isotype control antibody or PBS-treated mice (**Fig. 4c**).

Chronic airway exposure to PGP causes inflammatory remodeling

Chronic airway inflammatory diseases like COPD manifest alveolar enlargement and right ventricular hypertrophy. To evaluate whether the presence and activity of PGP in inflammatory situations can initiate a cascade of events culminating in pathology, we chronically administered PGP or PBS to the airways of mice and evaluated clinical parameters of lung pathology.

We treated C57 BL/6 mice with 250 μg PGP by direct airway instillation twice weekly for 12 weeks. We evaluated lungs and hearts 2 weeks after the last exposure for pathological changes. **Figure 5** shows micrographs of representative lung sections taken from PBS-treated control (**Fig. 5a**) and PGP-treated (**Fig. 5b**) mice. We observed enlargement of alveoli, as the mean alveolar linear intercept (Lm) was significantly increased (by 21%, $P < 0.05$) in PGP-exposed mice (**Fig. 5c**); these changes are similar to those reported for C57 BL/6 mice exposed to smoke from two cigarettes daily 6 d per week for 6 months[27]. BALB/c mice showed statistically significant but less substantial increases in Lm after 8 weeks of PGP treatment (**Supplementary Fig. 3** online). BALB/c and C57 BL/6 mice also showed increased levels of vascular endothelial growth factor (VEGF) in the lung (data not shown) and right ventricular hypertrophy (**Fig. 5d** and **Supplementary Fig. 3** online) in response to PGP treatment; at present, we do not know whether this effect is a consequence of PGP's recruitment of PMNs or a secondary effect of PGP. It remains to be tested whether specific inhibition of PGP by monoclonal antibody 9A4 would prevent the inflammatory and structural changes seen in response to long-term exposure to peptide.

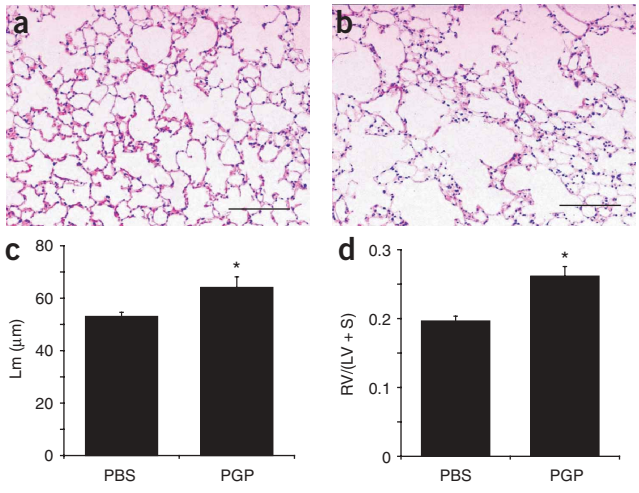

Figure 5 Extended exposure to PGP causes alveolar enlargement and right ventricular hypertrophy. C57Bl/6 mice were intranasally treated with PGP (250 μg in PBS) or PBS twice weekly for 12 weeks, and evaluated 2 weeks after the last treatment. H&E-stained lung sections from PBS- (**a**) and PGP-treated mice (**b**) were evaluated for alveolar enlargement. Scale bar, 100 μm. (**c**) A 21% increase in Lm in the PGP-treated group ($^*P = 0.021$). (**d**) Right ventricular (RV) mass is proportionally greater than the rest of the lower heart (that is, the left ventricle (LV) and the septum (S)) for PGP-treated mice than for PBS-treated controls (22%, $^*P = 0.025$).

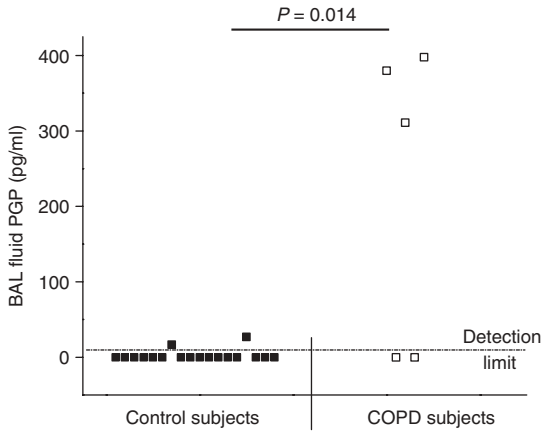

Figure 6 BAL fluid samples from individuals with COPD contain elevated levels of PGP. BAL samples from humans were assayed for PGP using ESI-LC-MS/MS. Incidence of PGP is greater among individuals with COPD (3 of 5) than controls (2 of 18, $P = 0.014$), and detected levels of PGP are higher in individuals with COPD (363) than controls (22; $P = 0.015$).

PGP is present in BAL fluids from people with COPD

To determine whether PGP is a marker of pathology in human disease, we screened for PGP in BAL fluid samples from individuals with COPD. Using the same ESI-LC-MS/MS method with more sensitive instrumentation, we could quantitatively detect as little as 10 pg/ml PGP (**Fig. 6**). Three of the five samples from individuals with COPD tested were positive for PGP, with concentrations averaging 363 pg/ml, whereas the 2 samples from the 18 control samples with signal above the detection limit averaged only 22 pg/ml. The difference in PGP concentration between positive samples of the groups was highly significant ($P < 0.01$ by unpaired *t*-test with Welch correction), whereas the incidence of PGP detection was also significantly different between the groups ($P = 0.014$ by Fisher exact test). Other important features of this study were that the three individuals with COPD who were positive for PGP also had evidence of emphysema by CT scan and lower mean FEV1 scores (50 ± 6% versus 62% predicted) than the two individuals with COPD who were negative for the peptide.

DISCUSSION

Neutrophil chemoattractant properties of PGP-containing peptides have been documented since 1970 (refs. 7,28). We report here for the first time that this activity occurs through the neutrophil CXC chemokine receptors. We also show that tissue breakdown after exposure to LPS causes generation of PGP *in vivo*. Furthermore, collagen-derived peptides in BAL fluids are active PMN chemoattractants, and specifically targeting these with monoclonal antibody 9A4 relieves the neutrophil burden in the lung 24 h after exposure to LPS to about the same extent as treatment with chemokine-specific monoclonal antibody. PGP exposure studies show that the novel activity of this peptide can recruit PMNs into airways and initiate inflammation, causing alveolar enlargement. Finally, the presence of PGP in samples from individuals with COPD suggests that collagen processing and the resulting recruitment of PMNs may actively drive the pathology of this disease.

Several ECM proteins contain the PGP motif, which is most abundant in collagen but is also present in collagen-like domains of elastin and surfactant proteins A and D. Because collagen normally forms a helical trimer, cleavage by collagenase (MMP-1 or MMP-9) exposes the normally hidden PGP-containing strands[19], unmasking proinflammatory activity of structural proteins. Generation of the tripeptide described here may require further cleavages by collagenases or gelatinases, and modification by acetylases present in inflammation. Because PGP is detected after early PMN infiltration, it is unclear whether neutrophil-derived enzymes are required for production of PGP, and the specific sequence of molecular events creating this chemoattractant remain unknown.

Macrophages release several MMP species after inflammatory stimuli, and their presence and activity correlate with COPD pathology[29]. Models of exposure to cigarette smoke show that both breakdown of ECM (by neutrophil or macrophage elastase) and accumulation of neutrophils are required for pathological change[30], and mice lacking either macrophage elastase[31] or neutrophil elastase[27] do not break down ECM and do not recruit PMNs into the lung, despite an intact chemokine signaling system. Our data suggest that PGP and related peptides are active in acute inflammation and may recruit cells in chronic situations where MMPs are upregulated and cells continue to infiltrate despite a lack of chemokine signal.

The basis for PGP's activity lies in its molecular similarity to the GP motif present in all ELR$^+$ CXC chemokines. Mutation or juxtaposition (GP to PG) of these residues in IL-8 render the molecule essentially nonfunctional[20]. This motif was suggested to be the probable receptor binding site in primary IL-8 studies[21], whereas other reports suggest that this motif initially binds the receptor, allowing cooperative binding between other parts of the ligand and receptor to efficiently transduce G-protein signaling[32]. This cooperativity probably accounts for the pharmacological differences between PGP and the chemokines, whose *in vitro* activities are optimal at micromolar and nanomolar concentrations, respectively. As seen with other peptides and cytokines[33–35], doses of PGP or chemokines required to overcome lung clearance mechanisms and observe airway inflammatory changes are nearly 1,000-fold higher than amounts in BAL fluids, whereas the dose ratio between PGP and chemokines is consistent between *in vivo* and *in vitro* studies. We thus consider PGP a partial agonist of chemokine receptors[36], which could be present and perhaps active in multiple inflammatory settings where matrix breakdown is occurring.

Antagonizing chemokines and leukotrienes incompletely block neutrophil chemotaxis to human COPD samples[37]. Detection of PGP in samples from individuals with COPD could explain residual chemotactic activity, and may account for long-term sequelae seen in chronic inflammation. Although the concentration of PGP in the BAL fluid is below its chemotactic threshold, it becomes more relevant when we account for the ~1:100 dilution of airway lining fluid by the lavage process reported in earlier human studies[25], placing the *in situ* concentration of diffusible PGP around 0.1 μM. Larger peptides containing the PGP sequence possess similar chemotactic activity[9,38] and could also contribute to overall chemotaxis, though such species have not been measured. Future longitudinal studies in humans for multiple PGP-related peptides, perhaps with breath-condensate samples[39], will probably best determine the contribution of this pathway to airway disease and use as a disease marker.

Clinical findings with IL-8–specific monoclonal antibodies[40] in individuals with COPD implies that cell trafficking is a realistic therapeutic target for inflammatory diseases. The activity of PGP as a PMN chemoattractant may represent another target. This idea is consistent with the protease-antiprotease hypothesis of airway diseases[41], and is corroborated by assertions that breakdown of ECM may be an important therapeutic target in chronic airway diseases[29], and that tissue damage is self-sustaining[42]. PGP signaling through CXCRs on neutrophils indicates that combining MMP blockade with chemokine receptor antagonism may dampen multiple

modalities of neutrophil recruitment in acute and chronic inflammation, and could potentially prevent the extensive tissue damage and remodeling seen in advanced disease.

METHODS

Reagents. We purchased peptides from Anaspec Inc., and checked them for purity by high-performance liquid chromatography and mass spectrometry–mass spectrometry (PLJ). IgG1, IgG2a, MIP-2–specific, KC-specific and CXCR-specific monoclonal antibodies and recombinant MIP-2 and KC and ELISA kits were from R&D Systems. The monoclonal antibody 9A4 was a gift from Pfizer's Global Research and Development. We purchased Cellgro standard solutions and media (trypsin-EDTA 0.1%, DMEM, Iscove media, PBS, HBSS) from University of Alabama at Birmingham (UAB) media services. BSA, LPS and Histopaque 1077 and 1062 were from Sigma, and recombinant human IL-8 was from Chemicon.

Mice. BALB/c, C57 BL/6J and *Cxcr2*$^{-/-}$ mice were from Jackson Labs. All *in vivo* experimental protocols were approved by the UAB Institutional Animal Care and Use Committee and Utrecht University Animal Care Committee.

***In vivo* administration.** We performed intratracheal administrations under halothane anesthesia in volumes of 50 µl. LPS was aerosolized with a Pari-LC nebulizer (PARI Respiratory Equipment) driven by compressed air, feeding a 10-L bottom-vented chamber (particle size, 2.5–3.1 µm; flow rate, 6 L/min).

Mouse BAL analysis. Immediately after mice were killed by intraperitoneal pentobarbital and bilateral thoracotomy, they were lavaged with four 1-ml collections of cold saline. We centrifuged cells, stained them and counted them by hemocytometry. Differential cytometry employed flow cytometry and dry-mount H&E staining (Fisher). We kept supernatants at 4 °C until analysis.

Lm measurements. After mice were killed, isolated left lungs were fixed in 25 cm-H_2O Carnoy fixative, paraffin-embedded and H&E stained; ten random fields were evaluated by microscopic projection onto a reference grid. We quantified alveolar wall–gridline intersections, and calculated average distance between alveolar walls (Lm)[43].

Right ventricular hypertrophy measurement. We removed right ventricles from lower heart after removal of atria. We weighed ventricles and septum after blotting and calculated the ratio of the weights as follows: (right ventricle)/(left ventricle + septum)[44] ratio.

Cells and cell lines. We isolated human PMNs by density centrifugation using Histopaque. We purchased HL-60 cells from the American Type Culture Collection and maintained them under recommended conditions and differentiated them into PMN-like cells by 96-h 1.3% DMSO incubation as previously described[45]. The expression of CXCR1 and CXCR2 was dependent on differentiation. We isolated mouse PMNs from bone marrow[46] and peritoneum[33] as previously described.

Chemotaxis assays. We placed indicated reagents in the bottom wells of a 3-µm 96-well polycarbonate filter plate (Millipore) in 150 µl DMEM and added 2×10^5 cells in 100 µl DMEM with 5% BSA to the top portion. We incubated the plate for 1 h at 37 °C in 5% CO_2 and removed the upper portion. Micrographs of migrated cells on the bottom plate were made with an Olympus IX70 microscope and Perkin Elmer Ultraview equipment and migration was standardized from cell counts such that chemotactic index = cells per high-powered field (experimental) / cells per high-powered field (media control), as previously described[47].

Superoxide measurements. We performed real-time detection of superoxide as previously described[48] with luminol, horseradish peroxidase and sodium azide with human PMNs in an Optocomp I Luminometer (MGM Instruments).

Flow cytometry. Mouse neutrophils from BAL or bone marrow were identified as GR-1$^+$Mac-1$^+$ cells[49] using monoclonal antibodies (Pharmingen) and a Becton Dickinson FACSCalibur flow cytometry system.

Radioligand competition assay. As previously described for IL-8 (ref. 50), we washed CXCR1 and CXCR2 (ref. 24) RBL transfectants, pooled and resuspended them at 5×10^6 cells/ml in 100 µl RPMI 1640 with 1% BSA and 0.5% HEPES and incubated them with unlabeled IL-8, PGP or PBS for 30 min at 22 °C before adding ^{125}I-radiolabeled IL-8 (specific activity, 1,500 Ci/mmol, Perkin Elmer) for 90 min at 4 °C. We counted cell pellets and supernatants separately in a Micromedic Systems 4/200 automatic gamma counter. We evaluated nonspecific binding with 100× unlabeled IL-8 and subtracted the value from the experimental values presented.

Human samples. Samples of human BAL fluid were obtained from the UAB Core Facility for Collection, Processing and Storage of Alveolar Fluid. This facility is approved by the UAB Institutional Review Board for Human Use. Samples of BAL fluid were collected with informed consent from each subject. Five samples were from individuals (two males, three females) with clinically diagnosed COPD whose FEV1 were below 62%. Emphysema was evaluated with computed tomography. Control samples of BAL fluid were from individuals who had undergone lung transplant ($n = 12$, samples from donor lung) or individuals with other diseases and without pulmonary infections ($n = 6$), including one each who had surfactant protein C deficiency, liver transplant, bone marrow transplant, Hodgkin disease and two leukemias.

ESI-LC/MS/MS. Mouse samples went through MDS Sciex (Applied Biosystems) with an API-300 and a Shimadzu high-performance liquid chromatographer (HPLC). HPLC used a 2.1 × 100 mm reverse-phase column (RP-300 Perkin Elmer) with 0–40% gradient of 0.1% formic acid and acetonitrile running at 0.2 ml/min for 8 min. Positive electrospray mass transitions were 312-112 and 312-140. Human samples went through the API-4000 Q-Trap.

Statistical analyses. We used InStat software (Graphpad). Two-tailed Student *t*-tests were used for simple significance testing, ANOVA for comparing three or more groups, and Fisher exact test for contingency table analyses. Means are presented ± s.e.m.; statistical significance is considered $P < 0.05$.

Note: Supplementary information is available on the Nature Medicine website.

ACKNOWLEDGMENTS

The authors acknowledge J. Downs (Pfizer Inc.) for the gift of the 9A4 monoclonal antibody, the laboratory of J. Oppenheim (US National Institutes of Health) for providing the CXCR-transfected cells, and P. O'Reilley, W. Bailey and K. Young for advice. We thank S. Parker of the University of Alabama at Birmingham (UAB) Core Facility for Collection, Processing and Storage of Alveolar Fluid for clinical samples and the UAB Mass Spectrometry Core Facility for sample analysis. This work was supported by US National Institutes of Health grants HL68806 (to J.E.B.), T32HL007553 (to B.D.N.), T32 GM63490 (to B.D.N.), T32 GM008361 (to N.M.W.) and F30 ES13874 (to N.M.W.).

COMPETING INTERESTS STATEMENT

The authors declare that they have no competing financial interests.

Published online at http://www.nature.com/naturemedicine/
Reprints and permissions information is available online at http://npg.nature.com/reprintsandpermissions/

1. Kobzik, L. The Lung. in *Robbins Pathologic Basis of Disease* (eds. Cotran, R.S., Kumar, V. & Collins, T.) (W.B. Saunders Company, Philadelphia, 1999).
2. Abraham, E., Carmody, A., Shenkar, R. & Arcaroli, J. Neutrophils as early immunologic effectors in hemorrhage- or endotoxemia-induced acute lung injury. *Am. J. Physiol. Lung Cell. Mol. Physiol.* **279**, L1137–L1145 (2000).
3. Rot, A. & von Andrian, U.H. Chemokines in innate and adaptive host defense: basic chemokinese grammar for immune cells. *Annu. Rev. Immunol.* **22**, 891–928 (2004).
4. Baggiolini, M., Dewald, B. & Moser, B. Human chemokines: an update. *Annu. Rev. Immunol.* **15**, 675–705 (1997).
5. Weathington, N.M. & Blalock, J.E. The biology of CXC chemokines and their receptors. in *Current Topics in Membranes* Vol. 55 (ed. Schwiebert, L.M.) 49–71 (Elsevier, New York, 2005).
6. Cacalano, G. *et al.* Neutrophil and B cell expansion in mice that lack the murine IL-8 receptor homolog. *Science* **265**, 682–684 (1994).
7. Chang, C. & Houck, J.C. Demonstration of the chemotactic properties of collagen. *Proc. Soc. Exp. Biol. Med.* **134**, 22–26 (1970).
8. Postlethwaite, A.E. & Kang, A.H. Collagen-and collagen peptide-induced chemotaxis of human blood monocytes. *J. Exp. Med.* **143**, 1299–1307 (1976).

9. Laskin, D.L., Kimura, T., Sakakibara, S., Riley, D.J. & Berg, R.A. Chemotactic activity of collagen-like polypeptides for human peripheral blood neutrophils. *J. Leukoc. Biol.* **39**, 255–266 (1986).
10. Senior, R.M. *et al.* Neutrophils show chemotaxis to type IV collagen and its 7S domain and contain a 67 kD type IV collagen binding protein with lectin properties. *Am. J. Respir. Cell Mol. Biol.* **1**, 479–487 (1989).
11. Pfister, R.R., Haddox, J.L., Sommers, C.I. & Lam, K.W. Identification and synthesis of chemotactic tripeptides from alkali-degraded whole cornea. A study of N-acetyl-proline-glycine-proline and N-methyl-proline-glycine-proline. *Invest. Ophthalmol. Vis. Sci.* **36**, 1306–1316 (1995).
12. Pfister, R.R., Haddox, J.L. & Sommers, C.I. Alkali-degraded cornea generates a low molecular weight chemoattractant for polymorphonuclear leukocytes. *Invest. Ophthalmol. Vis. Sci.* **34**, 2297–2304 (1993).
13. Pfister, R.R., Haddox, J.L. & Sommers, C.I. Injection of chemoattractants into normal cornea: a model of inflammation after alkali injury. *Invest. Ophthalmol. Vis. Sci.* **39**, 1744–1750 (1998).
14. Riley, D.J. *et al.* Neutrophil response following intratracheal instillation of collagen peptides into rat lungs. *Exp. Lung Res.* **14**, 549–563 (1988).
15. Foronjy, R.F., Okada, Y., Cole, R. & D'Armiento, J. Progressive adult-onset emphysema in transgenic mice expressing human MMP-1 in the lung. *Am. J. Physiol. Lung Cell. Mol. Physiol.* **284**, L727–L737 (2003).
16. Selman, M. *et al.* Tobacco smoke-induced lung emphysema in guinea pigs is associated with increased interstitial collagenase. *Am. J. Physiol.* **271**, L734–L743 (1996).
17. Corbel, M. *et al.* Repeated endotoxin exposure induces interstitial fibrosis associated with enhanced gelatinase (MMP-2 and MMP-9) activity. *Inflamm. Res.* **50**, 129–135 (2001).
18. Hauert, A.B., Martinelli, S., Marone, C. & Niggli, V. Differentiated HL-60 cells are a valid model system for the analysis of human neutrophil migration and chemotaxis. *Int. J. Biochem. Cell Biol.* **34**, 838–854 (2002).
19. Downs, J.T. *et al.* Analysis of collagenase-cleavage of type II collagen using a neoepitope ELISA. *J. Immunol. Methods* **247**, 25–34 (2001).
20. Clark-Lewis, I., Dewald, B., Loetscher, M., Moser, B. & Baggiolini, M. Structural requirements for interleukin-8 function identified by design of analogs and CXC chemokine hybrids. *J. Biol. Chem.* **269**, 16075–16081 (1994).
21. Baldwin, E.T. *et al.* Crystal structure of interleukin 8: symbiosis of NMR and crystallography. *Proc. Natl. Acad. Sci. USA* **88**, 502–506 (1991).
22. Lee, Y.C. *et al.* NMR conformational analysis of cis and trans proline isomers in the neutrophil chemoattractant, N-acetyl-proline-glycine-proline. *Biopolymers* **58**, 548–561 (2001).
23. Jones, S.A., Wolf, M., Qin, S., Mackay, C.R. & Baggiolini, M. Different functions for the interleukin 8 receptors (IL-8R) of human neutrophil leukocytes: NADPH oxidase and phospholipase D are activated through IL-8R1 but not IL-8R2. *Proc. Natl. Acad. Sci. USA* **93**, 6682–6686 (1996).
24. Feniger-Barish, R., Yron, I., Meshel, T., Matityahu, E. & Ben-Baruch, A. IL-8-induced migratory responses through CXCR1 and CXCR2: association with phosphorylation and cellular redistribution of focal adhesion kinase. *Biochemistry* **42**, 2874–2886 (2003).
25. Rennard, S.I. *et al.* Estimation of volume of epithelial lining fluid recovered by lavage using urea as marker of dilution. *J. Appl. Physiol.* **60**, 532–538 (1986).
26. Otterness, I.G. *et al.* Detection of collagenase-induced damage of collagen by 9A4, a monoclonal C-terminal neoepitope antibody. *Matrix Biol.* **18**, 331–341 (1999).
27. Shapiro, S.D. *et al.* Neutrophil elastase contributes to cigarette smoke-induced emphysema in mice. *Am. J. Pathol.* **163**, 2329–2335 (2003).
28. Pfister, R.R., Haddox, J.L., Lam, K.W. & Lank, K.M. Preliminary characterization of a polymorphonuclear leukocyte stimulant isolated from alkali-treated collagen. *Invest. Ophthalmol. Vis. Sci.* **29**, 955–962 (1988).
29. Belvisi, M.G. & Bottomley, K.M. The role of matrix metalloproteinases (MMPs) in the pathophysiology of chronic obstructive pulmonary disease (COPD): a therapeutic role for inhibitors of MMPs? *Inflamm Res.* **52**, 95–100 (2003).
30. Churg, A. *et al.* Acute cigarette smoke-induced connective tissue breakdown requires both neutrophils and macrophage metalloelastase in mice. *Am. J. Respir. Cell Mol. Biol.* **27**, 368–374 (2002).
31. Hautamaki, R.D., Kobayashi, D.K., Senior, R.M. & Shapiro, S.D. Requirement for macrophage elastase for cigarette smoke-induced emphysema in mice. *Science* **277**, 2002–2004 (1997).
32. Clark-Lewis, I. *et al.* Structure-activity relationships of chemokines. *J. Leukoc. Biol.* **57**, 703–711 (1995).
33. Adair-Kirk, T.L. *et al.* A site on laminin alpha 5, AQARSAASKVKVSMKF, induces inflammatory cell production of matrix metalloproteinase-9 and chemotaxis. *J. Immunol.* **171**, 398–406 (2003).
34. Tomkinson, A. *et al.* A murine IL-4 receptor antagonist that inhibits IL-4- and IL-13-induced responses prevents antigen-induced airway eosinophilia and airway hyperresponsiveness. *J. Immunol.* **166**, 5792–5800 (2001).
35. Grunig, G. *et al.* Requirement for IL-13 independently of IL-4 in experimental asthma. *Science* **282**, 2261–2263 (1998).
36. Goodman, L.S., Hardman, J.G., Limbird, L.E. & Gilman, A.G. *Goodman & Gilman's The Pharmacological Basis of Therapeutics,* 10th Ed. (McGraw-Hill, New York, 2001).
37. Beeh, K.M. *et al.* Neutrophil chemotactic activity of sputum from patients with COPD: role of interleukin 8 and leukotriene B4. *Chest* **123**, 1240–1247 (2003).
38. Haddox, J.L. *et al.* Bioactivity of peptide analogs of the neutrophil chemoattractant, N-acetyl-proline-glycine-proline. *Invest. Ophthalmol. Vis. Sci.* **40**, 2427–2429 (1999).
39. Horvath, I., Hunt, J. & Barnes, P.J. Exhaled breath condensate: methodological recommendations and unresolved questions. *Eur. Respir. J.* **26**, 523–548 (2005).
40. Mahler, D.A., Huang, S., Tabrizi, M. & Bell, G.M. Efficacy and safety of a monoclonal antibody recognizing interleukin-8 in COPD: a pilot study. *Chest* **126**, 926–934 (2004).
41. Turino, G.M. The origins of a concept: the protease-antiprotease imbalance hypothesis. *Chest* **122**, 1058–1060 (2002).
42. Senior, R.M. & Anthonisen, N.R. Chronic obstructive pulmonary disease (COPD). *Am. J. Respir. Crit. Care Med.* **157**, S139–S147 (1998).
43. Vernooy, J.H., Dentener, M.A., van Suylen, R.J., Buurman, W.A. & Wouters, E.F. Long-term intratracheal lipopolysaccharide exposure in mice results in chronic lung inflammation and persistent pathology. *Am. J. Respir. Cell Mol. Biol.* **26**, 152–159 (2002).
44. Nishimura, T. *et al.* Simvastatin rescues rats from fatal pulmonary hypertension by inducing apoptosis of neointimal smooth muscle cells. *Circulation* **108**, 1640–1645 (2003).
45. Collins, S.J., Ruscetti, F.W., Gallagher, R.E. & Gallo, R.C. Terminal differentiation of human promyelocytic leukemia cells induced by dimethyl sulfoxide and other polar compounds. *Proc. Natl. Acad. Sci. USA* **75**, 2458–2462 (1978).
46. Boxio, R., Bossenmeyer-Pourie, C., Steinckwich, N., Dournon, C. & Nusse, O. Mouse bone marrow contains large numbers of functionally competent neutrophils. *J. Leukoc. Biol.* **75**, 604–611 (2004).
47. Miller, A.P. *et al.* Estrogen modulates inflammatory mediator expression and neutrophil chemotaxis in injured arteries. *Circulation* **110**, 1664–1669 (2004).
48. Wymann, M.P., von Tscharner, V., Deranleau, D.A. & Baggiolini, M. Chemiluminescence detection of H2O2 produced by human neutrophils during the respiratory burst. *Anal. Biochem.* **165**, 371–378 (1987).
49. Lagasse, E. & Weissman, I.L. Flow cytometric identification of murine neutrophils and monocytes. *J. Immunol. Methods* **197**, 139–150 (1996).
50. Clark-Lewis, I., Schumacher, C., Baggiolini, M. & Moser, B. Structure-activity relationships of interleukin-8 determined using chemically synthesized analogs. Critical role of NH2-terminal residues and evidence for uncoupling of neutrophil chemotaxis, exocytosis, and receptor binding activities. *J. Biol. Chem.* **266**, 23128–23134 (1991).